ADVANCED FUNCTIONAL MATERIALS

DOI: 10.1002/adfm.200600068

Double-Inverse-Opal Photonic Crystals: The Route to Photonic Bandgap Switching**

By *Tilmann Ruhl*,* *Peter Spahn*, *Christian Hermann*, *Cecile Jamois*, and *Ortwin Hess**

Photonic crystals with a complete bandgap can stop the propagation of light of a certain frequency in all directions. We introduce double-inverse-opal photonic crystals (DIOPCs) as a new kind of optical switch. In the DIOPC, a movable, weakly scattering sphere is embedded within each pore of the inverse-opal photonic crystal lattice. Switching between a diffusive reflector and a photonic crystal environment is experimentally demonstrated. Theory shows that a complete bandgap can be realized that can be opened or closed by moving the spheres. This functionality opens up new possibilities for the control of light emission and propagation. The close link and interaction between the chemical synthesis and the computational design and analysis underlines the interdisciplinary focus of this report.

1. Introduction

Since John[1] and Yablonovitch[2] first introduced a novel concept for the localization of photons in dielectric media in 1987, considerable effort has been devoted to realizing photonic crystals that consist of dielectric structures with a periodicity on the order of the wavelength of light. Indeed, photonic crystals offer exciting opportunities for manipulating and controlling light,[3–5] which promise numerous applications, such as in optical waveguides, telecommunication devices, chemical and biological sensing, and solar cells. The periodic dielectric structure of a photonic crystal may, inside a limited photonic bandgap (PBG), lead to the confinement of light in specific directions (partial PBG) or even to the complete suppression of light propagation in all directions (complete PBG). In general, a complete bandgap can only be obtained in three-dimensional (3D) photonic crystals. The first successful realization of a material exhibiting a complete PBG, albeit in the microwave regime, was achieved by skillful oblique drilling of holes in a wafer, yielding a face-centered-cubic (fcc) lattice of nonspherical voids.[6] In the optical-wavelength regime, the most widely studied 3D photonic crystals are opal-based structures, since they can be synthesized quite easily by colloidal self-assembly.[7–13] In particular, inverse opals, which usually consist of spherical air voids arranged in a matrix in the form of an fcc lattice, can exhibit a complete bandgap if the refractive index of the backbone material is larger than 2.8.[14] This has already been experimentally demonstrated, e.g., in a silicon inverse opal yielding a complete bandgap in the infrared.[9]

However, the most exciting potential of photonic crystals lies in the possibility to impart functionality to the materials. Functional devices require tunable photonic crystals, or structures that allow complete switching of the bandgap. Early pioneering theoretical calculations demonstrated the possibility of tuning the PBG in silicon inverse opals by changing the molecular orientation of nematic liquid crystals that were to be partially infiltrated into the pores of an inverse-opal photonic crystal.[15] Unfortunately, the proposed setup has proven difficult to realize experimentally since—following the theoretical proposal—only the internal surfaces of the crystal were to be impregnated by the liquid-crystal molecules.[16] Additionally, the strong molecular alignment and the interaction of the liquid-crystal molecules with the surface of the silicon backbone,[17] which were not taken into account in the theoretical study,[15] may affect the tuning process.

Here we report the realization of a new type of opal-based photonic crystal, the double-inverse-opal photonic crystal (DIOPC), and show that it has the potential for PBG switching. The DIOPC is constituted of an inverted-opal backbone, in which each air pore is partially filled with a small silica sphere. As we will discuss, this structure allows for very novel PBG switching processes.

The article is organized as follows: After an overview of the fabrication process, we will present two ways of switching the optical properties of the DIOPC. The first process will lead to switching from diffusive to photonic behavior by infiltration of the structure, whereas the second one will open up the possibility to completely switch the entire PBG of the DIOPC on or off.

[*] Dr. T. Ruhl, P. Spahn
German Institute for Polymers
Schloßgartenstr. 6, 64289 Darmstadt (Germany)
E-mail: truhl@dki.tu-darmstadt.de
Prof. O. Hess, Dr. C. Hermann, Dr. C. Jamois
Advanced Technology Institute
School of Electronics and Physical Sciences, University of Surrey
Guildford, GU2 7XH (UK)
E-mail: o.hess@surrey.ac.uk

[**] This work was partially supported by the German Federal Ministry of Education and Research (FKZ: 13N8278). We are grateful to P. Göppert (NaWoTec GmbH), H. Winkler (Merck KGaA), and S. Hartmann for their assistance with the SEM images.

© 2006 WILEY-VCH Verlag GmbH & Co. KGaA, Weinheim
WILEY InterScience DISCOVER SOMETHING GREAT

2. Results and Discussion

2.1. Fabrication

The common route in the preparation of inverse-opal photonic crystals comprises the self-assembly of monodisperse colloidal spheres into an fcc lattice by controlled drying (vertical deposition).[12] The interstices of the spheres are filled by an inorganic material, either by chemical vapor deposition (CVD) or by chemical bath deposition, before final removal of the colloidal crystalline template.[10,13] The resulting inverse opals consist of an fcc arrangement of spherical air voids in an inorganic backbone. The voids are connected by small cylindrical channels that are a result of the contact points of the spheres in the lattice. The lattice spacing depends on the size of the initial colloids.

The preparation of the novel structure of double-inverse opals also follows this synthetic route, but starts from silica/polymer core/shell spheres that are absolutely uniform in size and in architecture, as shown in Figure 1. Monodisperse silica particles (radius of silica particles, $r_{silica} = 50$–150 nm) were prepared by a modified Stöber process in ethanol according to a previously reported procedure,[18] and their surfaces were functionalized by methacryloxypropyltrimethoxysilane (MEMO) in order to make them compatible with the polymer.[19] The particles were then transferred into an aqueous dispersion medium and, finally, they were covered with a shell of poly(methyl methacrylate) (PMMA) in a seeded emulsion polymerization.[20] This synthetic route for silica/polymer core/shell particles has been reported earlier,[21,22] but so far no homogeneous particles—uniform in size and in architecture—could be obtained. In addition to the desired core/shell particles, the dispersions always contained some defect particles, like purely polymeric particles[21] (Fig. 1a) or particles containing several silica cores covered with one common polymer shell[22] (Fig. 1b). Dispersions containing such defect particles—even in low concentrations—cannot be used for colloidal self-assembly since the defects frustrate the development of ordered structures. We therefore changed several aspects of the synthetic conditions. To functionalize the surface of the silica particles MEMO was added to the ethanolic dispersions at defined water and ammonia concentrations. The mixture was heated to 60 °C and stirred for one hour before the ammonia was removed at reduced pressure. Then the water was removed by azeotropic distillation while the volume was kept constant by continuous addition of absolute ethanol. According to a previous publication[19] precondensates of MEMO are first formed, which are then deposited on the surfaces of the spheres as the water is removed. This ensures that the particles are covered with a thick layer of the functionalizing agent. The particles were transferred to an aqueous dispersion media by adding a solution of sodium dodecyl sulfate (SDS) in water and removing ethanol by azeotropic distillation. The particles therefore always remained in a dispersing agent, which ensured that no irreversible agglomeration took place. Finally, they were concentrated to a solid content of 13 wt %. After the addition of Dowfax 2A1 as a surfactant, the dispersion was heated to 75 °C and a solution of sodium peroxodisulfate was added. Polymerization was started after 20 min by dropping in a monomer emulsion containing the monomers, water, and emulsifiers. The dropping rate was optimized in such a way that the amount of added monomer was equal to the amount of monomer which was converted by the reaction. By this starved-feed process, polymerization can be controlled in a much better way than in the batch process described in a previous report,[21] since the concentration of surfactant and monomer can be kept as low as possible at any stage of the reaction. With this optimized synthesis the formation of defect particles can be avoided completely (Fig. 1c).

Coating can be performed with various polymers like polyacrylates, polymethacrylates, or polystyrene and its derivatives. PMMA was chosen because of its glass-transition temperature of 120 °C and low decomposition temperature of 220 °C.

The dispersions were used without further purification to prepare colloidal crystals by vertical deposition on a microscope slide (Fig. 2). The transmission spectra of the colloidal crystal shows the (111) stop band, as well as signals from higher-energy bands, proving the high quality of the opal structure.

Titania or tin disulfide was grown in the voids of the opaline template by CVD. In the case of titania, the samples were placed in a stream of dry nitrogen that was subsequently loaded with water or titanium tetrachloride. Titania was grown from the surfaces of the spheres. The procedure was repeated three to four times to obtain a high filling ratio. The CVD process was studied in more detail using silicon tetrachloride for the deposition of silica,[23] and was proven to yield more homogeneous samples than infiltration via sol–gel precursors.

In the case of tin disulfide, the samples were first loaded with tin tetrachloride and then with hydrogen sulfide according to a previous report.[24] The PMMA layer of the core/shell particles was removed by calcination in air at 240 °C, yielding the DIOPC structure. The temperature needed to be controlled precisely since

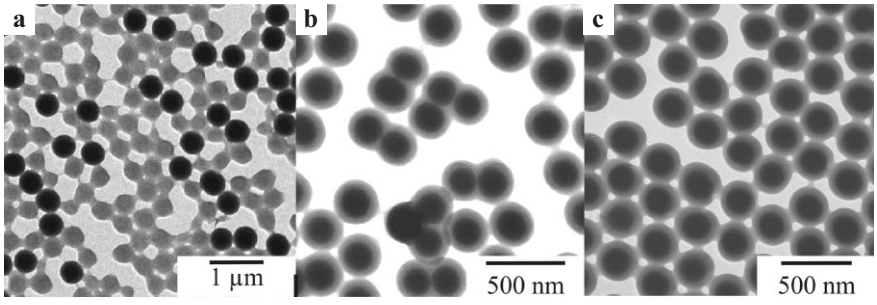

Figure 1. Transmission electron microscopy (TEM) images of silica/polymer core/shell particles: a) purely polymeric particles next to uncoated silica spheres; b) dispersion containing defect particles with several silica spheres covered with one common polymer shell; c) dispersion without any defect particles produced when the synthetic conditions are optimized.

© 2006 WILEY-VCH Verlag GmbH & Co. KGaA, Weinheim

ADVANCED FUNCTIONAL MATERIALS

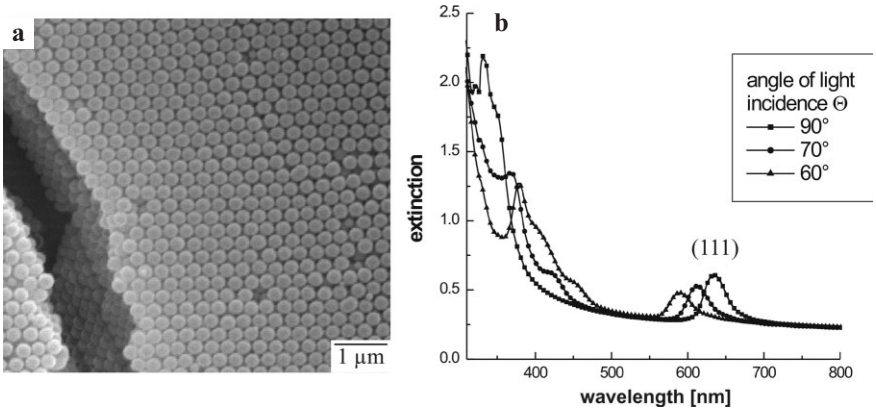

Figure 2. Colloidal crystal from silica/polymer core/shell spheres: a) Scanning electron microscopy (SEM) image of the (111) face; b) UV-vis spectra of the colloidal crystalline film at different angles of incidence ($r_{silica} = 95$ nm, $r_{particle} = 145$ nm).

higher temperatures led to conversion of tin disulfide to tin dioxide. Figure 3a shows a standard titania inverse opal prepared by this route using a dispersion of pure PMMA spheres. Figures 3b and c show typical examples of the DIOPC structure, the former with a titania backbone and the latter with a tin disulfide backbone.

The material parameters of the DIOPC can be adjusted precisely. The size of the silica spheres can be controlled by the modified Stöber process. The ratio of pore diameter to the sphere diameter in the DIOPC depends on the thickness of the polymeric layer in the core/shell particles, which can be controlled precisely by the amount of polymerized monomer. The size of the channels depends on the temperature during the process of vertical deposition (35 °C in Figs. 3a and c, 55 °C in Fig. 3b). At higher drying temperatures the PMMA shells of the hybrid particles are sintered, which enlarges the connecting channels.

The embedded silica spheres strongly modify the optical properties of the original inverse-opal photonic crystals and open up new design possibilities. The optical properties depend on the refractive index of the inorganic backbone and the size of the interconnecting channels, as well as the size, position, and distribution of the silica spheres within the pores. This allows for the realization of diverse tuning or switching processes. In the following, two examples are discussed in detail: the switching of the optical properties between a diffusive and a photonic behavior, and the switching of the complete PBG of the structure.

2.2. Switching Between Diffusive and Photonic Behaviors

In this first case, we consider a DIOPC consisting of silica spheres ($n_{silica} = 1.44$) and of a backbone material with a moderate refractive index like titania ($n_{titania} = 2.6$). The silica spheres are confined to the volume of each pore but are randomly distributed inside the pores, as shown in Figure 3b. The ordered titania backbone of the DIOPC should give rise to a photonic stop band. However, because of the moderate refractive index of the titania backbone, this stop band is strongly disturbed by the random distribution of the weakly scattering silica spheres. This disturbance can easily be removed by infiltration of the DIOPC with a material that has a refractive index matching that of the silica spheres, in order to obtain (by masking) a structure similar to that of a standard titania inverse opal, wherein the pores are completely filled with silica. Since a sufficient refractive index contrast between the infiltrated pores and the ordered titania backbone in the infiltrated DIOPC still exists, this structure should show a pronounced stop band. Therefore, this simple infiltration process should allow for the switching of the behavior of the DIOPC from diffusive to photonic. In order to demonstrate this behavior experimentally, we infiltrated the structure with water (whose refractive index almost matches that of the silica spheres) and performed transmission and reflectivity measurements on the sample before and after infiltration, as presented in Figure 4.

For the unfilled titania–silica DIOPC, a (111) stop band should be centered at a wavelength of about 505 nm. The stop band is almost completely suppressed by the randomly distributed silica spheres and can therefore only be observed as a small dip in transmission (Fig. 4a) and a small peak in reflection (Fig. 4b). This proves that the DIOPC behaves, in this case, like a diffusively scattering material.

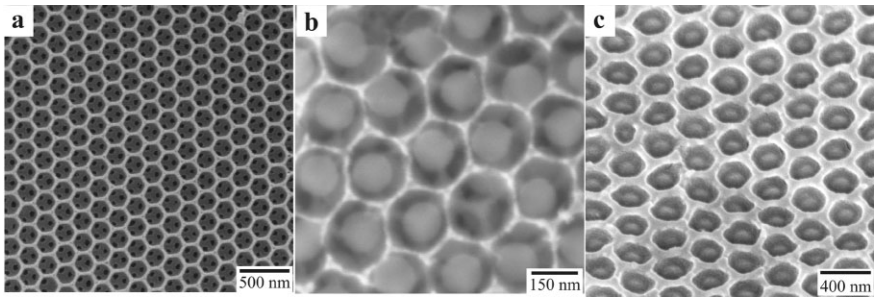

Figure 3. SEM image of the (111) face. a) Titania inverse opal ($a_{111} = 210$ nm, $r_{cyl} = 20$ nm; r_{cyl} is the radius of the cylindrical channels connecting the spheres, see Figure 5). b) Titania–silica double-inverse opal ($a_{111} = 210$ nm, $r_{pore} = 108$ nm, $r_{silica} = 60$ nm, $r_{cyl} = 35$ nm). c) Tin disulfide–silica double-inverse opal ($a_{111} = 260$ nm, $r_{pore} = 160$ nm, $r_{silica} = 80$ nm).

© 2006 WILEY-VCH Verlag GmbH & Co. KGaA, Weinheim

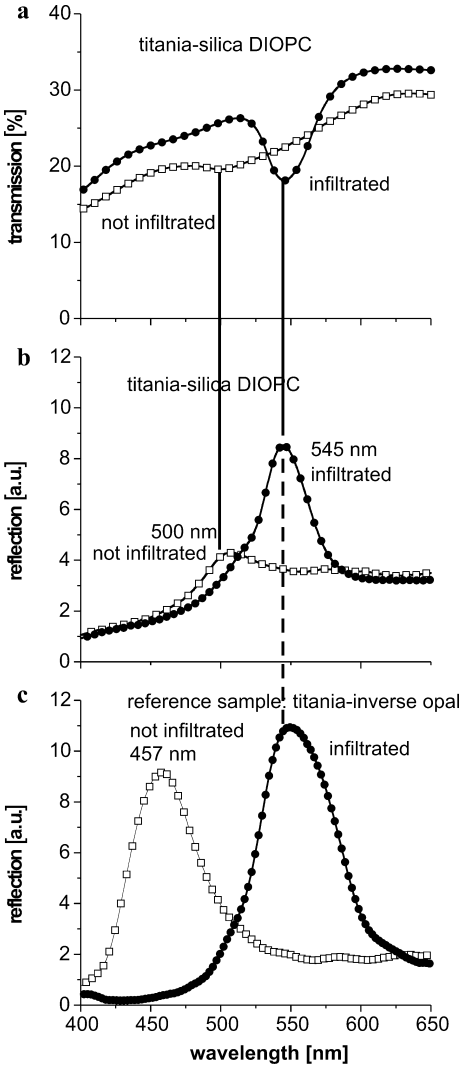

Figure 4. Optical characterization of inverse-opal photonic crystals. a) Transmission spectra of a titania–silica DIOPC not infiltrated (□) and infiltrated (●) with water at a sample tilt of 0°. b) Reflectivity measurement of the same sample using a fiber spectrometer at a sample tilt of 0°. c) Reflectivity measurement of a standard titania inverse opal, as a reference, at a sample tilt of 0°. Expected positions of the stop bands are marked with lines.

After infiltration with water, the DIOPC shows a pronounced (111) stop band centered at a wavelength of 545 nm, which is similar to the infiltrated titania inverse-opal reference (Fig. 4c) since the disturbance of the silica spheres is optically removed. This is, to our knowledge, the first demonstration of switching between a diffusive and a photonic environment by a simple infiltration process.

So far, it has only been possible to shift the wavelength of the stop band by infiltration of inverse opals,[25] as shown in Figure 4c. However, the switching effect can only be observed if the radius of the silica spheres is within a certain size range, $r_{silica} = 0.5\,r_{pore}$ to $0.85\,r_{pore}$, where r_{pore} is the radius of the pore. If the silica spheres are too small, they cannot effectively disturb the light scattering of the backbone. In this case, the DIOPC behaves similarly to an inverse opal of air spheres in titania with a stop band at about 457 nm, as shown in the reference measurement in Figure 4c. If the silica spheres are too large, they almost completely fill the whole pore volume and there are only slight fluctuations of the positions possible. In this case, the DIOPC behaves similarly to an inverse opal made of silica spheres in titania, and no switching behavior can be observed by infiltration of the structure with water.

2.3. PBG Switching

In order to demonstrate the possibility of switching the complete bandgap of the DIOPC, we need to consider a backbone material with a higher refractive index. Indeed, the refractive index of the titania is too low to open up a complete bandgap in the titania–silica DIOPC, discussed in the previous section, independently of other material parameters such as the sphere radii. This is different for a tin disulfide–silica DIOPC. Tin disulfide has a refractive index of 3.2 (at 700 nm) and is transparent above its absorption edge at 550 nm.[24] Our theoretical calculations show that, for certain sets of parameters, a complete bandgap opens up between the eighth and the ninth band of the DIOPC. In the following, we will show that it is possible to completely open and close this bandgap by shifting the position of the silica spheres within the pores. Note that, in this case, the position of the silica spheres is assumed to be well defined, contrary to being in random positions discussed in the previous section. The theoretical results presented below have been obtained by plane-wave calculations,[26] where the inverse-opal structure has been modeled as closed-packed spheres ($r_{pore} = 0.354\,a$), connected by cylindrical channels with radius r_{cyl}, as shown in Figure 5a for the experimental system and Figure 5b for the theoretical model. Besides the structural parameters r_{cyl} and r_{silica}, we now also have to consider the position of the silica spheres within the pores. One must be

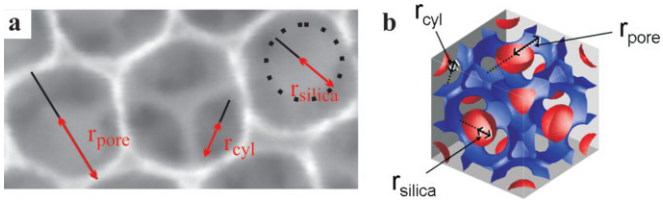

Figure 5. Geometrical parameters of the DIOPC for the calculation of the photonic properties: a) Experimental system (SEM image, extracted from Figure 3b). The size of r_{cyl} can be determined in a pore where the silica sphere dropped out. b) Model for theoretical calculations with centered silica spheres (blue: SnS_2; red: SiO_2).

aware that a collective shift of the silica spheres in a certain direction may break particular symmetries of the crystal and, therefore, the degeneracy of high-symmetry points. This has to be taken into account when determining the position of the complete bandgap. Here we restrict ourselves to the case where the silica spheres are completely shifted in the (111) and (100) directions, and are in contact with the tin disulfide wall. Since the (111) shift is the "natural" position because of the

© 2006 WILEY-VCH Verlag GmbH & Co. KGaA, Weinheim

ADVANCED FUNCTIONAL MATERIALS

fabrication process, and the (100) shift promises the largest modification of the air band (the upper band edge is related to a mode with a *k*-vector pointing in the (100) direction), this is an obvious choice for tuning the bandgap and for potential "switching states". A more comprehensive analysis of the parameter space will be presented elsewhere.

Figure 6a shows the gap size for the two switching states depending on the size of the silica spheres for $r_{cyl} = 0.1\, r_{pore}$. The PBG is, as expected, larger for a (111) shift and decreases with r_{silica}. Consequently, there is a small range of r_{silica}, between

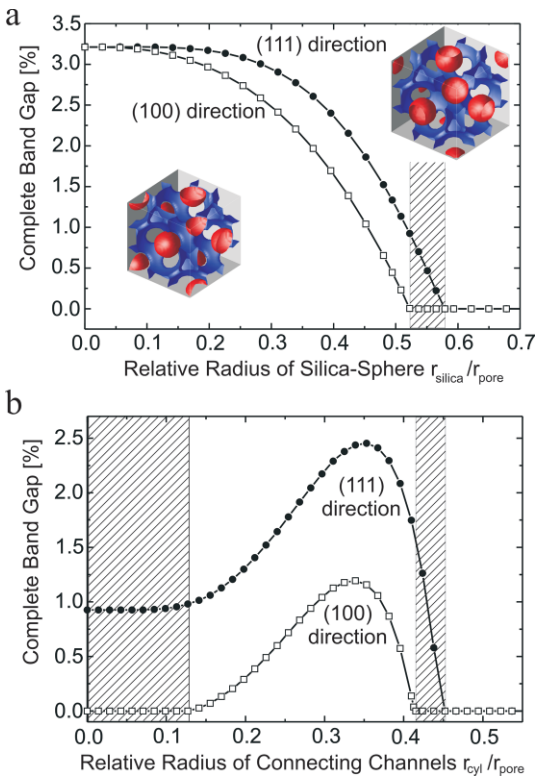

Figure 6. Bandgap size for two switching states: spheres shifted in the (111) direction (●) and the (100) direction (□). Dependence of bandgap size on a) r_{silica} for $r_{cyl} = 0.1\, r_{pore}$ and b) r_{cyl} for $r_{silica} = 0.525\, r_{pore}$. Parameter ranges in which a complete switching is possible are marked in boxes.

$0.52\, r_{pore}$ and $0.565\, r_{pore}$, where the gap is closed for the (100) shift and still open for the (111) shift. In a second step, we investigated the influence of r_{cyl} on the complete bandgap. Since r_{silica} can be controlled precisely in the material fabrication, we choose $r_{silica} = 0.525\, r_{pore}$ (yielding an optimum switchable PBG of about 0.9 %) to investigate the influence of r_{cyl} (Fig. 6b). We see that in this case there are two regions where the bandgap may be completely switched from open to closed: the first one occurs for $r_{cyl} < 0.127\, r_{pore}$, yielding a gap size of about 0.9 %, and the second one for $0.415\, r_{pore} < r_{cyl} < 0.452\, r_{pore}$, yielding a gap size of up to 1.5 %. The first region is very stable with respect to variations in r_{cyl}. It will therefore be of great experimental interest, since it is more difficult to precisely control r_{cyl} during the fabrication process. However, in the second region, the switchable PBG is larger.

Note that although the structure of the tin disulfide–silica DIOPC shown in Figure 3c could possibly yield a tunable bandgap as discussed above, it does not yet fulfill all conditions required for the experimental realization of complete bandgap switching. For this ultimate goal, the lattice constant of the DIOPC is currently still too small so that the complete PBG is expected at wavelengths below the absorption edge of tin disulfide and, therefore, is not experimentally observable. Shifting the complete PBG to higher wavelengths requires a synthesis of larger inorganic–polymeric hybrid particles of high quality. Furthermore, collective shifting of the inner spheres requires inorganic cores that are addressable by external electric or magnetic fields. We are currently optimizing these two aspects and it seems realistic that both issues can be addressed technologically in the near future.

3. Conclusions and Outlook

We have presented the realization of double-inverse-opal photonic crystals, a new type of 3D photonic crystal consisting of an inverted-opal backbone with a small silica sphere in each pore. The double-inverse-opal structure allows for the realization of different switching processes. In particular, the optical properties of the structure can be switched from diffusive to photonic behavior by a simple infiltration process, provided the refractive index contrast between the silica spheres and the backbone material is not too high (e.g., titania backbone). On the other hand, we have shown that if the backbone material has a refractive index that is high enough to open a complete bandgap (e.g., tin disulfide), the main potential of the DIOPC is the possibility to open or close a complete bandgap in this 3D photonic crystal by applying external fields. This may help to realize functional photonic crystals for dynamic control of spontaneous emission or to realize photonic crystal waveguides that would allow for the design of adaptive 3D optical integrated circuits.

4. Experimental

Ammonia (25 wt %, aqueous solution), sodium dodecyl sulfate (SDS), potassium hydroxide, titanium tetrachloride, and tin tetrachloride were obtained from VWR Scientific Products, tetraethylorthosilicate (TEOS) and methacryloxypropyltrimethoxysilane (MEMO) from ABCR (Karlsruhe, Germany), sodium peroxodisulfate from Fluka, Dowfax 2A1 from Dow Chemical, hydrogen sulfide from Messer Griesheim, and methyl methacrylate (MMA) from BASF. MMA was distilled before use.

Silica particles were prepared following the procedure described by Graf and van Blaaderen [18] in ethanol with a final SiO_2 solid content of 2.5 wt %, a water concentration of 2 mol L^{-1}, and an ammonia concentration of 0.69 mol L^{-1}. 2.25 L of this ethanolic dispersion was mixed with 4 mL MEMO diluted with 6 mL ethanol. The mixture was slowly heated to 60 °C and stirred for 1 h before the pressure was reduced to 300 mbar (1 mbar = 100 Pa). In the beginning the ammonia was removed, together with the azeotrope of ethanol and water. Later on, the residual water was removed at 200 mbar by azeotropic distillation of ethanol/water at 60 °C, while the volume was kept constant by continuous addition of absolute ethanol. When the dispersion was free of water, the volume was reduced to 0.5 L and stirring was continued

© 2006 WILEY-VCH Verlag GmbH & Co. KGaA, Weinheim

for an additional 90 min at 60 °C. To transfer the particles into an aqueous dispersion medium, a solution of 0.1 g SDS in 200 g water was added and ethanol was removed by azeotropic distillation, while the volume was kept constant by continuous addition of water. When the dispersion was free of ethanol, the volume was reduced to 300 mL with a solid content of 13 wt %. The functionalized silica particles had a size of $r_{silica} = 50$ to 150 nm and a standard deviation of 3–5 % of the average sphere diameter, depending on the number of growth steps.

Polymerization was carried out in a reaction vessel with a reflux condenser and a propeller stirrer. A solution of 0.1 g Dowfax 2A1 in 20 mL water was added to the dispersion before it was heated to 75 °C and a solution of 0.1 g sodium peroxodisulfate in 10 mL water was added. After 20 min, a monomer emulsion consisting of 14 g MMA, 56 g water, 0.15 g KOH, and 0.1 g Dowfax 2A1 was fed dropwise over a period of 150 min. After stirring for 30 min (without monomer addition), a solution of 0.03 g sodium peroxodisulfate in 10 mL water was added for complete conversion. Afterwards, a second monomer emulsion containing 0.22 g SDS, 98 g water, 65 g MMA, and 0.15 g KOH was added dropwise over a period of 180 min. To complete polymerization, the dispersion was stirred for another 60 min. The thickness of the polymer shell could be varied by changing the amounts of the added monomer emulsions.

Colloidal crystals were prepared from the diluted particle dispersions (0.05 wt %) by vertical deposition on a microscope slide. The dispersions were dried in a period of 3–5 days at a temperature of 35 or 55 °C, while the samples were placed in a slight air stream.

To fill the interstices with titania, the samples were placed in a stream of dry nitrogen for 5 min in a Schlenk tube of a vacuum line before the nitrogen stream was guided through 5 mL of titanium tetrachloride for 3 min. The vacuum line was cleaned of excess titanium tetrachloride with pure nitrogen for 2 min before the stream was guided through 5 mL of distilled water. The procedure was repeated three to four times to obtain a high filling ratio. In the case of tin disulfide the samples were loaded with tin tetrachloride first and then with hydrogen sulfide according a reported procedure [23]. The PMMA layer of the hybrid particles was removed by calcination at 240 °C in air.

TEM samples were prepared by drying the diluted dispersions (0.01 wt %) on a carbon-supported copper grid. A Zeiss EM 910 operating at an acceleration voltage of 100 kV was used for obtaining the TEM images. SEM images of the DIOPC were obtained on a LEO 1560 XB operating at 15 kV, with a sample distance of 8 mm to the incident electron beam.

Transmission UV-vis spectra were recorded using a Perkin Elmer Lambda 40 spectrometer. The microscope slides were placed on a rotatable sample holder. UV-vis spectra in reflection were recorded using a fiber spectrometer (AvaSpec 1024, Avantes; light source FO 6000, World Precision Instruments). The spectrometer was calibrated with a white standard (Spectralon white plate, Labsphere). For infiltration with water a drop was placed at the border of the DIOPC layer covering the microscope slide. The drop distributed homogenously by capillary action.

Received: August 24, 2005
Final version: January 11, 2006
Published online: March 21, 2006

[1] S. John, *Phys. Rev. Lett.* **1987**, *58*, 2486.
[2] E. Yablonovitch, *Phys. Rev. Lett.* **1987**, *58*, 2059.
[3] J. D. Joannopoulos, R. D. Meade, J. N. Winn, in *Photonic Crystals—Moulding the Flow of Light*, Princeton University Press, Princeton, NJ **1995**.
[4] A. Birner, R. B. Wehrspohn, U. M. Gösele, K. Busch, *Adv. Mater.* **2001**, *13*, 377.
[5] J. D. Joannopoulos, P. R. Villeneuve, S. Fan, *Nature* **1997**, *386*, 143.
[6] E. Yablonovitch, T. J. Gmitter, K. M. Leung, *Phys. Rev. Lett.* **1991**, *67*, 2295.
[7] O. D. Velev, T. A. Jede, R. F. Lobo, A. M. Lenhoff, *Nature* **1997**, *389*, 447.
[8] J. E. G. Wijnhoven, W. L. Vos, *Science* **1998**, *281*, 802.
[9] A. Blanco, E. Chomski, S. Grabtchak, M. Ibisate, S. John, S. W. Leonard, C. Lopez, F. Meseguer, H. Miguez, J. P. Mondia, G. A. Ozin, O. Toader, H. M. van Driel, *Nature* **2000**, *405*, 437.
[10] N. Tetreault, A. Mihi, H. Míguez, I. Rodríguez, G. A. Ozin, F. Meseguer, V. Kitaev, *Adv. Mater.* **2004**, *16*, 346.
[11] L. Bechger, W. L. Vos, *Chem. Mater.* **2004**, *16*, 2425.
[12] P. Jiang, K. Bertone, K. S. Hwang, V. L. Colvin, *Chem. Mater.* **1999**, *11*, 2132.
[13] C. F. Blanford, H. Yan, R. C. Schroden, M. Al-Daous, A. Stein, *Adv. Mater.* **2001**, *13*, 401.
[14] K. Busch, S. John, *Phys. Rev. E* **1998**, *58*, 3896.
[15] K. Busch, S. John, *Phys. Rev. Lett.* **1999**, *83*, 967.
[16] E. Yabolonovitch, *Nature* **1999**, *401*, 539.
[17] D. Kang, J. E. Maclennan, N. A. Clark, A. A. Zakhidov, R. H. Baughman, *Phys. Rev. Lett.* **2001**, *86*, 4052.
[18] C. Graf, A. van Blaaderen, *Langmuir* **2002**, *18*, 524.
[19] P. Philipse, A. Vrij, *J. Colloid Interface Sci.* **1989**, *128*, 121.
[20] T. Ruhl, P. Spahn, H. Winkler, G. P. Hellmann, *Proc. SPIE-Int. Soc. Opt. Eng.* **2004**, *5450*, 67.
[21] J. L. Luna-Xavier, A. Guyot, E. Bourgeat-Lami, *J. Colloid Interface Sci.* **2002**, *250*, 82.
[22] K. Zhang, H. Chen, X. Chen, Z. Chen, Z. Cui, B. Yang, *Macromol. Mater. Eng.* **2003**, *288*, 380.
[23] H. Miguez, N. Tetreault, B. Hatton, S. M. Yang, D. Perovic, G. A. Ozin, *Chem. Commun.* **2002**, 2736.
[24] M. Müller, R. Zentel, T. Maka, S. G. Romanov, C. M. Sotomayor Torres, *Adv. Mater.* **2000**, *12*, 1499.
[25] C. F. Blanford, R. C. Schroden, M. Al-Daous, A. Stein, *Adv. Mater.* **2001**, *13*, 26.
[26] S. G. Johnson, J. D. Joannopoulos, *Opt. Express* **2001**, *8*, 173.

© 2006 WILEY-VCH Verlag GmbH & Co. KGaA, Weinheim